Proceedings of the XVII ECSMGE-2019
Geotechnical Engineering foundation of the future
ISBN 978-9935-9436-1-3

doi: 10.32075/17ECSMGE-2019-0537

XVII European Conference on Soil Mechanics and Geotechnical Engineering
ECSMGE 2019 Reykjavik

Failure mechanisms developed in rock masses under circular footing

Les mécanismes de défaillance développés sous la semelle circulaire

Svetlana Melentijevic
Faculty of Geology, University of Complutense, Madrid, Spain

Ana Alencar, Rubén Galindo
ETSI Caminos, Canales y Puertos, Polytechnic University of Madrid, Madrid, Spain

ABSTRACT: The bearing capacity of the circular footing on rock mass is studied in this paper. The finite difference method is applied for the analysis of the bearing capacity for a wide variety of types and states of rock masses under the assumption of the Hoek and Brown material, using axisymmetric model to simulated the circular footing. The results are analysed based on a sensitivity study varying 4 parameters (foundation width, rock material constant (m_o), uniaxial compressive strength and geological strength index). The bearing capacity obtained numerically is compared with results estimated by published analytical methods. To analyse the failure mechanisms developed under the footing the model is also performed under plane strain conditions, and the difference between the wedge developed under the strip and circular footing is presented.

RÉSUMÉ: Cet article présente une étude sur la capacité portante de la masse rocheuse pour une semelle circulaire. La méthode des différences finies est appliquée pour l'analyse de la capacité portante d'une grande variété de types et états de masses rocheuses, dans l'hypothèse du critère de rupture de Hoek et Brown et utilisant le modèle axisymétrique pour simuler la semelle circulaire. Les résultats sont analysés sur la base d'une étude de sensibilité dans laquelle quatre paramètres influents dans la capacité portante varient (mo, largeur de la semelle, GSI et RC). La capacité portante obtenue numériquement est comparée aux résultats estimés par les méthodes publiées. Pour analyser les mécanismes de défaillance développés sous la semelle, le modèle est également réalisé pendant la condition de déformation plane et la différence entre le coin développé sous la semelle filante et circulaire est constatée.

Keywords: bearing capacity; circular footing; finite difference method; rock mass; failure mechanism.

1 INTRODUCTION

Among the influencing factors of the ultimate bearing capacity of shallow foundation on rock mass it can been emphasized that the footing shape was not studied a lot (Carter and Kulhawy (1988), Clausen (2013), Ramamurthy (2014), Chakraborty and Kumar (2015) and Keshavarz and Kumar (2017)).

Based on the Hoek and Brown failure criterion (1980), Carter and Kulhawy (1988) proposed two formulations to estimate the ultimate bearing capacity for strip and circular footing. Both equations are based on lower bound solution adopting the hypothesis of weightless rock.

However, according to Clausen (2013) no systematic results of bearing capacity of circular footings resting on a generalized Hoek–Brown material have previously been presented in the literature. This author claims that there is no correction factor that allows to estimate how much load a circular footing support more than a strip footing as a consequence of only geometry. Therefore, the shape factor for circular footing was proposed by the same author that allows to estimate the bearing capacity of a circular footing on rock mass by multiplying the uniaxial compressive strength for intact rock mass (UCS) by this coefficient.

Chakraborty and Kumar (2015) emphasizes that there is no literature about the influence of the footing shape on the bearing capacity of rock mass and proposes a methodology to determine the bearing capacity of a circular footing over rock mass based on the quasi lower bound limit analysis, in conjunction with the finite element method and the non-linear optimization.

Ramamurthy (2014) suggests that the square or the circular footing resting on the rock mass support 20% more load than the strip footing of the same width. This author recommends to estimate the bearing capacity by the Carter and Kulhawy (1988) formulation for strip foundation and increase this results in 20% to obtain the bearing capacity for square or circular footing.

The formulation of the bearing capacity proposed by Carter and Kulhawy (1988) (equation (1)) and bearing capacity charts for circular footings based on the GSI system proposed by Clausen (2013) introduces a bearing capacity factor ($N_{\sigma C}$) which makes the failure pressure proportional to the uniaxial compressive strength of the rock (UCS).

$$P_h = [s^a + (m_b \cdot s^a + s)^a] \cdot UCS \qquad (1)$$

In the present paper these failure mechanisms and the results obtained in the calculation of the bearing capacity for a shallow foundation on a rock mass are analysed. The comparison of the numerical results was developed as function of the bearing capacity factor ($N_{\sigma C}$), with those proposed by Carter and Kulhawy (1988) and Clausen (2013).

The graphic outputs of the displacements developed below the footing are presented and used to understand the differences between the failure mechanisms developed under the strip and circular footing.

2 NUMERICAL ANALYSIS

A total of 192 cases have been numerically performed, varying the geomechanical properties of the rock mass according to the Hoek and Brown failure criterion (2002) (m_o, UCS and GSI) and the foundation width (B).

Table 1. Summary of the parameters adopted.

m_o	B (m)	UCS (MPa)	GSI
5	4.5	5	10
12	11	10	50
20	16.5	50	85
32	22	100	

Numerical calculations were developed by the finite difference code FLAC employing 2-D models and applying the plane-strain condition to represent a strip footing and the axisymmetry condition to simulate a circular footing (Figure 1). The axisymmetric model uses a cylindrical coordinate system that allows to represent objects with axial symmetry, as is the case of a circular footing. In the case of the plane-strain condition, a symmetrical model is used, where only half of the strip footing is represented. The axisymmetric grid is viewed as a unit-radian sector (FLAC, 2007). The boundaries of both models are located at a distance that does not interfere in the result. In the numerical model the vertical load is directly applied to the nodes (ground surface) so that the characteristics of the foundation and the interaction with the ground surface do not influence the result. The mesh is shown in Figure 2, being more discretized in the area located under the foundation. The rock mass is considered under the assumption of the weightless rock mass. In all simulations the associative flow rule is adopted.

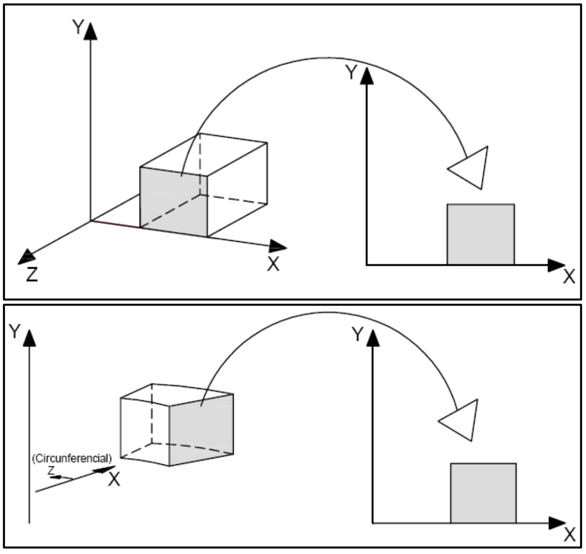

Figure 1. Plane-strain and axisymmetry conditions (modified from FLAC manual (2007)).

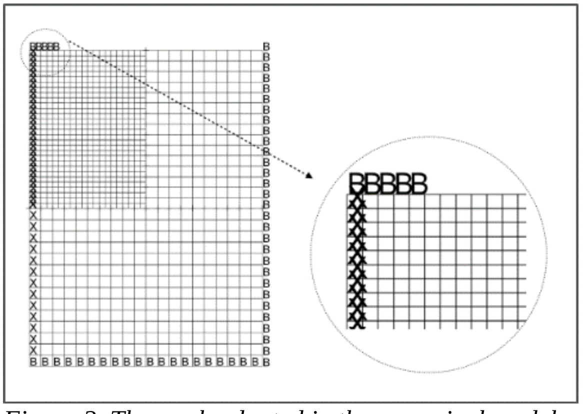

Figure 2. The mesh adopted in the numerical model.

Numerically it is assumed that the bearing capacity is reached when the continuous medium does not admit more load, due to development of the internal failure mechanism. In FLAC the load is applied through velocity increments, and the bearing capacity is determined from the relation between stresses and displacements of one of the nodes (in this case the central node of the foundation is considered).

A convergence study is carried out consisting in the analysis of values of the bearing capacity obtained under different increments of the velocity that is used, with the decrease in the value of velocity increments the result converges towards the final value by the upper limit in the theoretical method. For each case with different combination of geometrical and geotechnical parameters (Table 1) a convergence study is carried out with different values of velocity increments.

On the other hand, it is important to note that in the numerical calculations the model is usually simplified by adopting a footing as a load (velocity increments) applied directly on the ground surface. Thus, it is not necessary to define strength parameters for the footing, neither for the interface between the ground and the structure. To simulate a perfectly smooth or rough interface, the nodes where the load is applied are loose or fixed, allowing or not the displacement.

It was studied through sensitivity analysis how each variable parameters (m_o, B, UCS and GSI) influenced the bearing capacity obtained numerically (P_{hFLAC}).

Figure 3 shows that the bearing capacity increases with the increment of the m_o. However, it is observed that cases with high values of m_o can also be associated with the low value of bearing capacity; where it can be concluded that the rock type does not define the range of values of the bearing capacity.

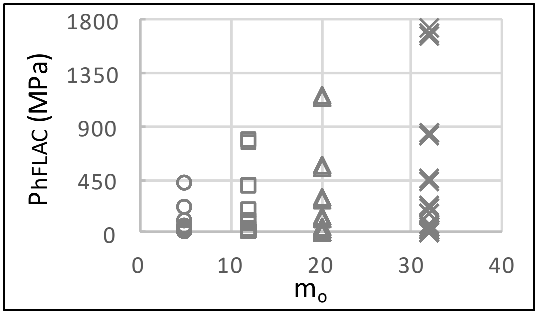

Figure 3. P_{hFLAC} in function of m_o.

Regarding Figure 4, a very slight increase in the results of bearing capacity obtained with increasing B can be observed. This small influence of the footing width in the bearing capacity is in accordance with the fact that the contribution of the self-weight is not considered.

In Figure 5 can be observed that the range of values of the bearing capacity is defined depending on the GSI value. The cases with low GSI are associated with low bearing capacity, concluding that the bearing capacity increases with the increment of the GSI. The other parameters studied (m_o, B and UCS) also have an influence on the value of the bearing capacity, but they do not define clear ranges of its variation as GSI.

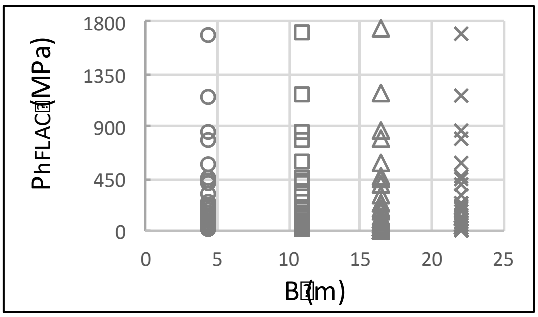

Figure 4. P_{hFLAC} in function of B.

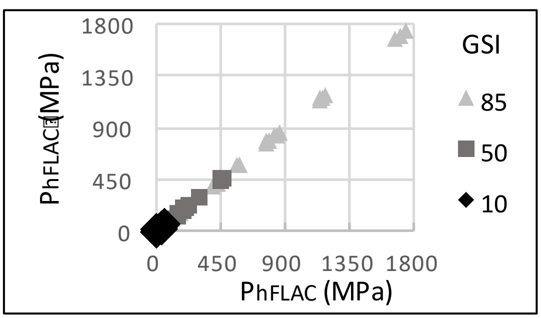

Figure 5. P_{hFLAC} in function of GSI.

Regarding the UCS parameter, it is observed that the numerical results present a direct correlation with the UCS, in the same way that the published analytical methods.

Table 2 shows two examples of the results of P_{hFLAC} where the correlation between P_{hFLAC} and the UCS is clearly demonstrated. For example, in case 2 the UCS has the double value in compariosn to the case 1, and the percentage variation of bearing capacity is the same.

Table 2. Results of P_{hFLAC} for different studied cases.

Cases				UCS	P_{hFLAC}
Nº	**m_o**	**B (m)**	**GSI**	**(MPa)**	**(MPa)**
1	12	16.5	10	5	0.9
2	12	16.5	10	10	1.77
3	12	16.5	10	50	9
4	12	16.5	10	100	18
5	20	11	85	5	57.6
6	20	11	85	10	115.5
7	20	11	85	50	575
8	20	11	85	100	1150

Confirming the previous statement, in Figure 6 can be observed that when the P_{hFLAC} is divided by the UCS (obtaining the bearing capacity factor $N_{\sigma C}$), the result is quite independent of the UCS value.

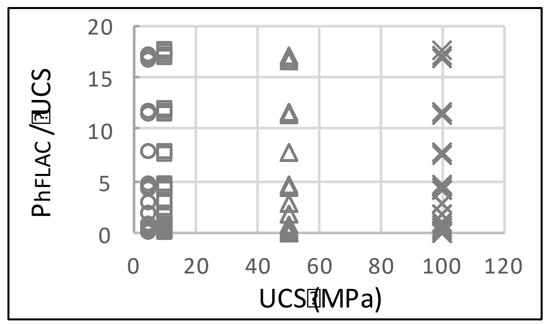

Figure 6. P_{hFLAC} in function of UCS.

3 RESULTS

The comparison between the results of the bearing capacity of rock mass obtained by different methods can be done through bearing capacity factor ($N_{\sigma C}$). This factor multiplied by the UCS allows to determine the bearing capacity.

Carter and Kulhawy (1988) and Clausen (2013) proposed a formulation to estimate $N\sigma c$ as function of the parameters used in the Hoek and Brown failure criterion; the results obtained numerically through the commercial code FLAC can also be expressed as a function of $N_{\sigma C}$.

The three calculation methods that are used are based on procedures / hypotheses that do not coincide in all aspects, therefore, it was expected that the results obtained would be similar, but not the same.

3.1 Comparation between $N_{\sigma C}$ values

The $N_{\sigma C}$ values obtained by these three methods are presented in Figure 7 and Figure 8, as function of the GSI and m_o, and employing the hypothesis of weightless rock mass and circular footing. There is a great difference between the value of $N_{\sigma C}$ estimated by the formulation proposed by Carter and Kulhawy (1988) and other results, that present very similar values being within the same order of magnitude.

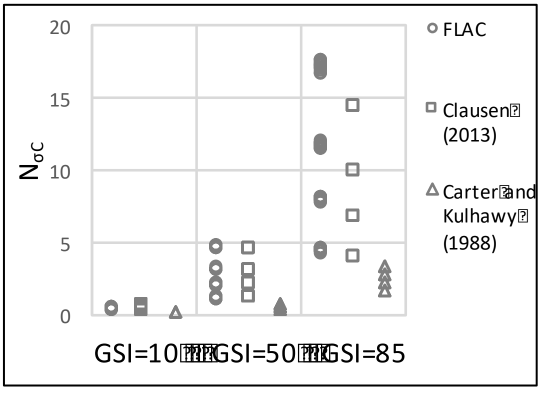

Figure 7. $N_{\sigma C}$ in function of GSI.

From Figure 7 it can be concluded that the dispersion range of results increase is associated with the increment of the GSI. It is emphasized that the P_{hFLAC} resemble to be a little higher than the bearing capacity estimated by Clausen (2013).

Confirming the previous statement, in Figure 7 can be observed that the GSI is the parameter that defines the range of the bearing capacity values.

Comparing $N_{\sigma C}$ calculated by FLAC with those estimated by method proposed by Clausen (2013), it can be observed that the greatest variation between the results occurs for greater values of GSI (i.e. GSI = 85), being FLAC results in the range of 10 to 17% higher than those obtained by the formulation proposed by Clausen (2013).

In relation to the results obtained by Carter and Kulhawy (1988) method, it is observed that the values obtained by the numerical method (P_{hFLAC}) can be up to 5 times greater.

Figure 8 shows that the $N_{\sigma C}$ depends on the rock type, following the trend that with the increase in the value of m_o, the $N_{\sigma C}$ value grows. It can be observed that the variation between the methods increase with the increment of m_o as well.

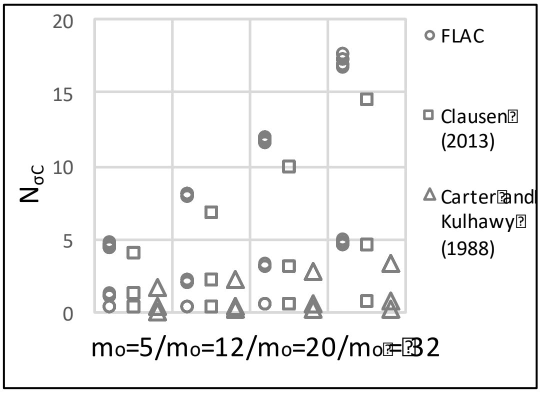

Figure 8. $N_{\sigma C}$ in function of m_o.

Finally, it can be concluded that the results obtained by the published analytical methods are lower than estimated numerically by FLAC. In relation to the influence of the geotechnical parameters the difference between the results increase for higher values of m_o and GSI.

3.2 Displacement analysis

In the numerical calculation to estimate the bearing capacity a stress path is formed until the failure is reached, taking into account the whole wedge of the ground below the foundation. Therefore, the graphic outputs of the displacements (horizontal and vertical) developed below the foundation are used to understand how the failure mechanism affected the results.

As it is generally known, the circular footing supports more load than the strip footing of the same width. This is due to the fact that the resistant mechanism of the circular footing is developed in 3-D. Under the plastic hypothesis a behavior of the strip footing can be simulated by several rectangles placed one next to each other, resulting in the overlapping of the bulbs of pressure reaching greater depths, these pressure bulbs depth differences can be expected at failure.

In both models (plane strain conditions and axisymmetric), the horizontal displacement decreases when the GSI increases (Figure 9). In axisymmetric model, in cases of low m_o, the horizontal displacement is concentrated close to the footing edge, and the shape of the displacement is similar to a pressure bulb. However, for high values of m_o the shape of horizontal displacements is more like a wedge, so the lateral boundary is more affected in these cases (Figure 10).

In relation to the vertical displacement, it is observed in both models that for high values of m_o and GSI the displacement limits (wedge) is best defined. Confirming the theory, the vertical displacement is deeper in the plane-strain model compared to the axisymmetric model (Figure 11).

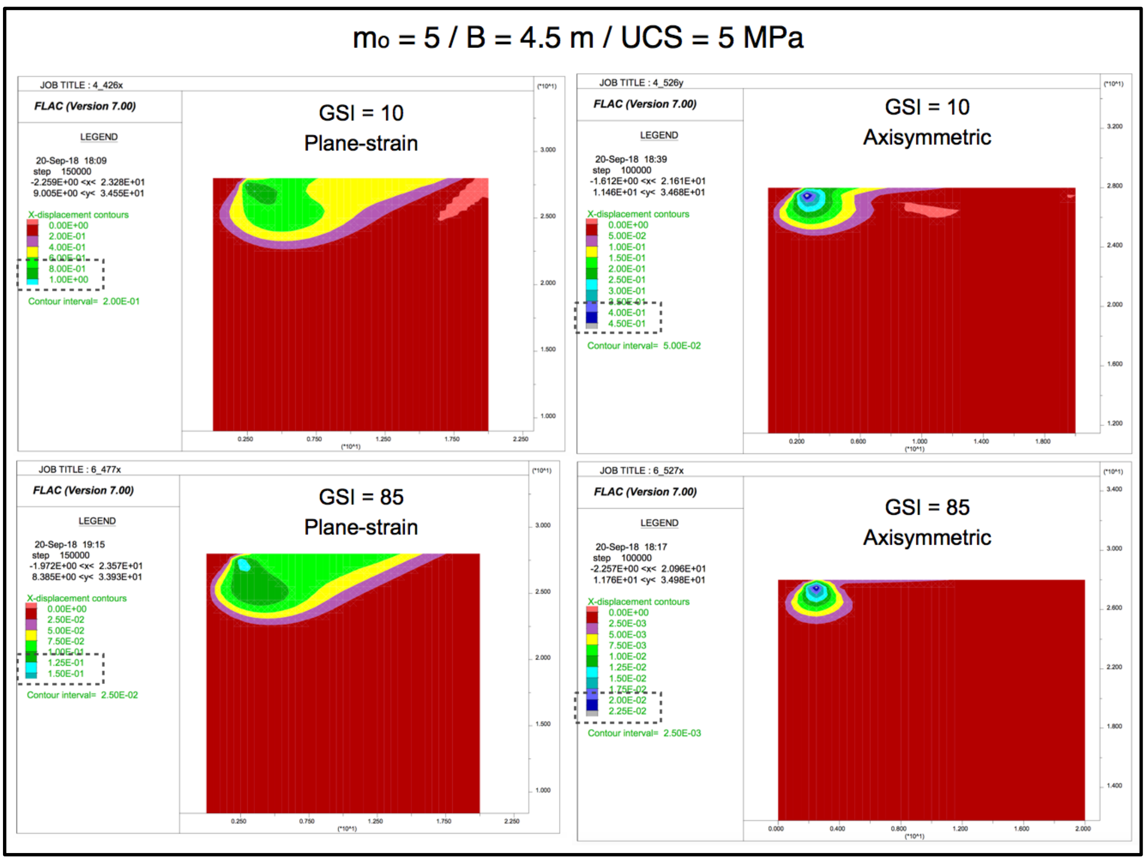

Figure 9. The variation of horizontal displacements under foundation as a function of GSI.

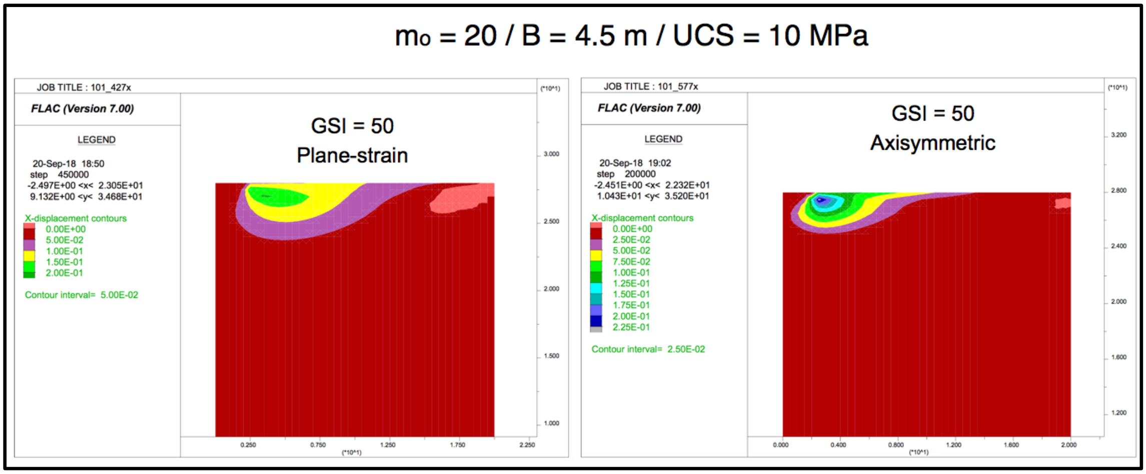

Figure 10. The variation of horizontal displacements under foundation.

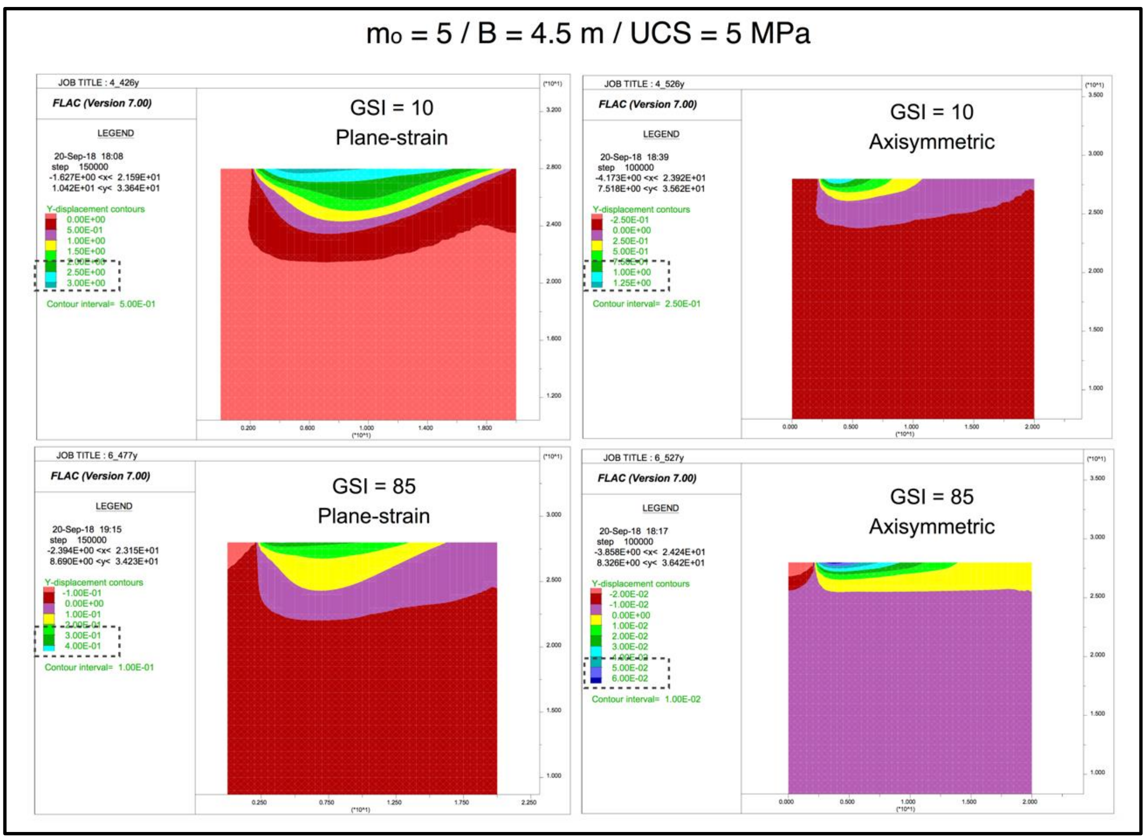

Figure 11. The variation of vertical displacements under foundation as a function of GSI.

4 CONCLUSIONS

Taking into account the comparison described in previous sections regarding numerical results of the bearing capacity of circular footing on rock masses obtained through the finite difference code FLAC and the other published analytical methods (Carter and Kulhawy (1988) and Clausen (2013)) the following can be concluded:

- The parameters that have most impact on the value of the bearing capacity factor ($N_{\sigma C}$) are m_o and GSI. The GSI defines the range of values of the $N_{\sigma C}$, low range of GSI is associated with the low $N_{\sigma C}$ and with the increase of the GSI the $N_{\sigma C}$ increases as well. On the other hand, it is also observed that the $N_{\sigma C}$ increases with the increment of the m_o.
- The parameters B and the UCS show a negligible influence on the bearing capacity factor ($N_{\sigma C}$) calculated numerically (the self-weight of the rock mass is not taken into account in the numerical model).
- The values of the bearing capacity factor ($N_{\sigma C}$) obtained by the commercial code FLAC are very similar to the proposed by Clausen (2013), presenting a maximum variation for GSI = 85, ranging from 10 to 17%. In relation to the results obtained by Carter and Kulhawy (1988) method, it is observed that the variation between P_{hFLAC} and the results can exceed 500%.
- The numerical analysis provides an insight into the failure mechanism developed under foundation in the rock mass observing the influence of different rock parameters on the bearing capacity of different foundation type (plane strain and axisymmetric conditions).
- The vertical displacement involves larger depth and volume under the foundation in the plane-strain model compared to the axisymmetric model for the same range of GSI values. In the same way, the horizontal displacement covers larger volume under the foundation in the rock mass under the plane strain condition.

5 REFERENCES

Carter J.P., Kulhawy F.H. (1988) Analysis and Design of Foundations Socketed into Rock, Report No. EL-5918. Empire State Electric Engineering Research Corporation and Electric Power Research Institute, New York, NY, p. 158.

Clausen J. (2013). Bearing capacity of circular footings on a Hoek–Brown material. International Journal of Rock Mechanics and Mining Sciences. 57. 34–41. 10.1016/j.ijrmms.2012.08.004.

Ramamurthy T. (2014) Engineering in rocks for slopes foundations and tunnels, 3rd ed., PHI Learning, Delhi

Chakraborty M., Kumar J. (2015) Bearing capacity of circular footings over rock mass by using axisymmetric quasi lower bound finite element limit analysis. Computers and Geotechnics, Volume 70, Pages 138-149, ISSN 0266-352X

Keshavarz A., Kumar J. (2017) Bearing capacity of foundations on rock mass using the method of characteristics. Int J Numer Anal Methods Geomech. 42:542-557.

Hoek E., Brown E.T. (1980) Empirical strength criterion for rock masses. J Geotech Eng Div ASCE. 106(9):1013–1035.

Hoek E., Carranza-Torres C., Corkum B. (2002) Hoek-Brown failure criterion – 2002 Edition. In Hammah R, Bawden W, Curran J, Telesnicki M, editors. Proceedings of NARMS-TAC 2002, Mining Innovation and Technology. Toronto – 10 July 2002, pp. 267–73.

FLAC (2007) User's Manual, Itasca Consulting Group Inc. Minneapolis.